SF2A 2025
A. Siebert, K. Baillié, M. Béthermin, F. Cantalloube, E. Josselin, N. Lagarde, J. Malzac, J. Richard, L. Selliez, O. Venot (eds)

STRUCTURE AND EVOLUTION OF THE ENVELOPES OF HOT WATER WORLDS

A. Aguichine[1], N. Batalha[1], J. Fortney[1], N. Nettelmann[1], J. Owen[3], E. Kempton[4], O. Mousis[5] and M. Deleuil[5]

Abstract. Sub-Neptunes represent compelling targets for being water worlds, exhibiting masses and radii that have been shown to match those of hypothetical water rich bodies. Recent work for irradiated water worlds predict that water in their envelope would be in the supercritical state, with steam atmospheres on top, which significantly alters the mass-radius relation. However, proper knowledge of the thermal state of the interior, which affects the predicted planetary radius, is elusive. This challenge is due to both lack of knowledge of laboratory data of material (equation of state and opacity), and difficulty to self-consistently model such interiors. Sub-Neptunes form with a huge energy reservoir, and cool down and contract over time, which has been incorporated into grids of H_2-rich sub-Neptune models, but never for water worlds. Here, we present a new model that accounts for the thermal contraction of water rich envelopes. This model combines an interior structure model with a radiative-convective steam atmosphere model, that are coupled through the heat lost from the planet's interior. The interior structure model uses the most up-to-date thermodynamic data for pure water substance, and the steam atmosphere model uses a new treatment for the opacity of water. This model provides new mass-radius relationships for water-rich hot sub-Neptunes through time, which reassesses the water content in sub-Neptunes. This allows us to quantify the range of radii accessible to such hypothetical planets.

Keywords: exoplanets, sub-Neptunes, water worlds, interior structure models, equations of state, planet evolution, atmospehre interior interaction

1 Introduction

The search for water rich exoplanets represents an overarching goal for astrobiology and the search for life. Over the past decade, extensive efforts were dedicated to the characterization of exoplanets. Precise measurements of exoplanet masses and radii can be used to constrain their bulk compositions using interior models (Seager et al. 2007; Fortney et al. 2007; Valencia et al. 2007). Sub-Neptunes, exoplanets with radii between $\sim$1.8 to $\sim$3.5 $R_\oplus$, are of particular interest because their densities are compatible with planets that have water rich interiors (Zeng et al. 2019; Mousis et al. 2020b).

Due to the proximity to their host star, known sub-Neptunes tend to have high equilibrium temperatures. In fact, most of them[*] are beyond the runaway greenhouse limit (Nakajima et al. 1992; Turbet et al. 2019), meaning that they cannot maintain liquid water oceans. Instead, such planets would have steam atmospheres on top of supercritical water envelopes (Mousis et al. 2020a). These considerations led to the development of coupled atmosphere-interior models to compute reliable mass-radius relationships for such planets (Turbet et al. 2020; Aguichine et al. 2021).

The purpose of this study is to implement the effect of the cooling of the interior so that the planetary radius becomes a functoin of time as well.

[1] Department of Astronomy and Astrophysics, University of California, Santa Cruz, CA, USA
[2] Imperial Astrophysics, Department of Physics, Imperial College London, Prince Consort Road, London SW7 2AZ, UK
[3] Department of Earth, Planetary, and Space Sciences, University of California, Los Angeles, CA 90095, USA
[4] Department of Astronomy, University of Maryland, College Park, MD 20742, USA
[5] Aix-Marseille Université, CNRS, CNES, Institut Origines, LAM, Marseille, France

[*]Almost 97% using the criteria from Turbet et al. (2019).

2 Methods

The interior structure model, based on the work of Brugger et al. (2017), is thoroughly described in Aguichine et al. (2021). For the sake of keeping our new results comparable with the older static model, we do not make any changes to the interior part of the model, and only review details that are relevant to the time-evolution modeling. The interior model iteratively solves the four classical equations describing the interior of a planet in 1D: mass conservation, hydrostatic equilibrium, adiabatic thermal gradient, and material equation of state (EOS). For the EOS of water, we use Mazevet et al. (2019).

Kempton et al. (2023) present a large grid of atmospheric structures for a wide variety of parameters: H_2O volume mixing ratio, surface gravity, intrinsic temperature, equilibrium temperature, and host star type; and associated transmission spectra. In this work, we limit ourselves to pure H_2O atmospheres, although the method presented here can be generalized to interiors where the atmosphere and envelope are mixtures of H_2O with H_2-He. The atmospheric structures are generated using the open-source package `HELIOS` (Malik et al. 2017, 2019a,b).

The interior and atmosphere models are connected at a surface pressure $P_\mathrm{b} = 1000$ bar. The time evolution is computed by integrating numerically the energy balance equation (Lopez et al. 2012; Lopez & Fortney 2014) $L_\mathrm{int} = -\frac{\mathrm{d}E_\mathrm{int}}{\mathrm{d}t}$, where $L_\mathrm{int} = 4\pi R_\mathrm{b} \sigma_\mathrm{SB} T_\mathrm{int}^4$ is the heat loss from he interior, and dE_int is the change of total energy in the interior with σ_SB the Stefan-Boltzmann constant. The energy sources account for cooling of the envelope, heat extracted from the core (iron core and mantle), gravitational energy, and energy produced by radiogenic heating in the interior. More details about the model can be found in Aguichine et al. (2025).

3 Results

In Figure 1, left panel, we shows the mass-radius relations for this model, hereafter A25 (Aguichine et al. 2025), the Aguichine et al. (2021) model, noted A21, and the 50% H_2O line from Zeng et al. (2019) noted Z19. Zeng et al. (2019) provide mass-radius curves for 50% and 100% H_2O planets for temperatures between 300 K and 1000 K. The Z19 model assumes an isothermal H_2O layer with a surface pressure of 1 mbar. The Zeng et al. (2016) (Z16) model provides a grid of planet radii as a function of mass and composition, but only at 300 bar of surface pressure. We also show the Lopez & Fortney (2014) (LF14) model, which is a model for planets with H_2-He envelopes. A grid of all evolutionary tracks are available on Zenodo `https://doi.org/10.5281/zenodo.15043384` (Aguichine et al. 2025), although we warn users about the limited validity range in equilibrium temperature space. For visualization in the mass-radius plane, the evolution tracks have been implemented in `mardigras` v2.3.1 (`https://github.com/an0wen/MARDIGRAS`) (Aguichine 2024, 2025).

The most important characteristic of an interior model is the reinterpretation of the bulk composition of exoplanets. We compare the bulk water content inferred from different interior models from the literature for 5 planets: TOI-776 b, GJ 9827 d, TOI-270 d, AU Mic c and GJ 1214 b. To infer the bulk water content of each planet, we adopt a Bayesian approach using the `emcee` sampler (Foreman-Mackey et al. 2013), and our results are summarized in Figure 2. As expected, Z16 consistently gives the highest estimate of the water mass fraction (WMF), and A21 the lowest. These results quantify the difference in inferred WMF when different assumptions are made for the thermodynamic state of the interior. We argue that out of the three models, A25 (Aguichine et al. 2025) corresponds to the most realistic thermodynamic state in the interior.

4 Conclusions

In this work, we computed the time evolution of Steam Worlds using an updated coupled atmosphere and interior model to better understand how composition affects the observed properties of sub-Neptunes. This framework combines an interior model of an Earth-like core with a pure water envelope (Aguichine et al. 2021), and a pure steam atmosphere on-top (Kempton et al. 2023) self-consistently. We refer the reader to Aguichine et al. (2025) for more details about the model.

We compared our model to previous work: Nettelmann et al. (2011), Aguichine et al. (2021), and Zeng et al. (2016, 2019); and found revised planetary radii thanks to new EOS and refined physical modeling. A grid of all evolutionary tracks are available on Zenodo `https://doi.org/10.5281/zenodo.15043384` (Aguichine et al. 2025), although we warn users about the limited validity range in equilibrium temperature space. For visualization in the mass-radius plane, the evolution tracks have been implemented in `mardigras` v2.3.1 (`https://github.com/an0wen/MARDIGRAS`) (Aguichine 2024, 2025).

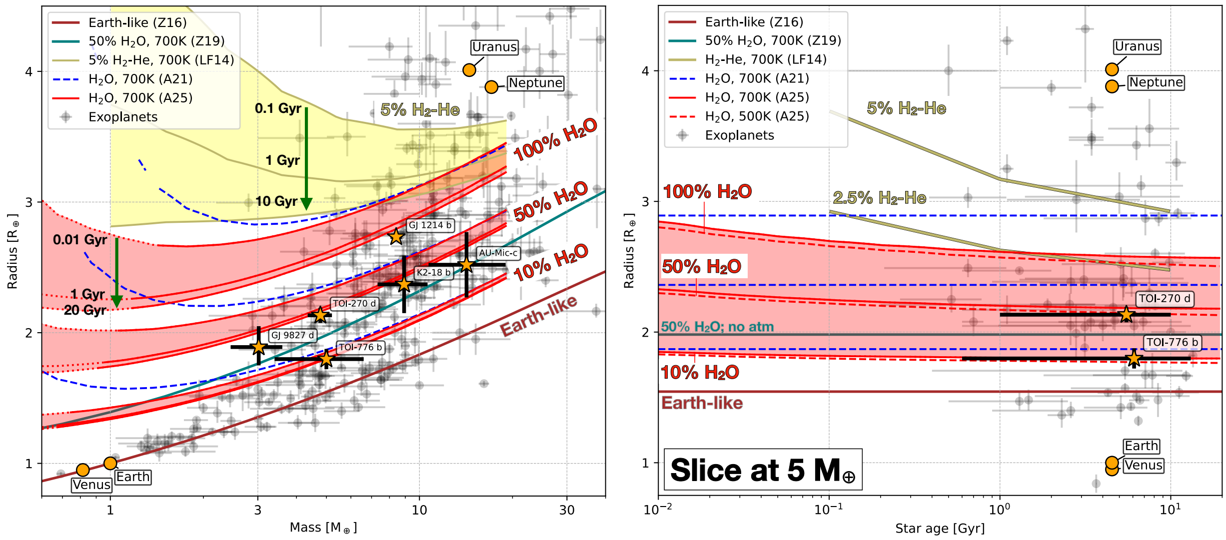

Fig. 1. Interior structure models in the mass-radius plane (left panel) and slice at 5 $M_\oplus$ in the radius-time plane (right panel): evolving steam worlds (red solid lines, A25), static steam worlds (blue dashed lines, A21), 50% isothermal steam worlds (teal solid line, Z19), Earth-like planets (brown solid line, Z16), and 5% H_2-He planets (yellow solid lines, LF14). Red and blue lines are shown for bulk water content of 10%, 50% and 100%, and for the red lines an M-type host star is assumed. Red and yellow shaded regions represent the span of evolution models of A25 and LF14, respectively. LF14 evolution is shown between 0.1 and 10 Gyr. A25 evolution is shown between 0.02 Gyr and 20 Gyr. All models assume an equilibrium temperature of 700 K, except the red dashed line in the right panel, which shows the A25 model at 500 K. Exoplanets properties are obtained from the NASA Exoplanet Archive, including 6 planets of interest shown with orange stars. Solar system planets are shown with orange circles.

Our new set of mass-radius relationships (left panel of Fig. 1) implies a re-interpretation of the bulk composition of sub-Neptunes. For older planets, the previous model (Aguichine et al. 2021) consistently overestimates the radius, and hence underestimates the bulk water content. On the other hand, the canonically used Zeng et al. (2016) model consistently underestimates the radius, and hence overestimates the bulk WMF. We also note that for most planets, there is still significant overlap in inferred WMF due to the large uncertainty on planet mass and radius. If the bulk WMF is known (from atmospheric measurements or theoretical predictions), in order to discriminate between interior structure models one needs mass and radius uncertainty comparable to that of TOI-270 d, respectively 19% and 8%. To reach this precision level, we advocate for more radial velocity observations using high precision facilities to constrain mass, e.g. with HARPS and ESPRESSO, and more transits using high sensitivity instruments to constrain radius, such as JWST, PLATO, and CHEOPS.

Although a pure steam atmosphere and envelope is a highly idealized case, this study showcases the main differences between the time evolution of H_2-dominated planets (Lopez & Fortney 2014; Tang et al. 2024) and steam worlds (this work), which is necessary to understand sub-Neptunes on a population level. We believe that this model pushes forward our understanding of planetary atmospheres and interiors, and refines the inference of the composition of sub-Neptunes. This study unveils possible links between the bulk composition of sub-Neptunes and the system's age, both of which are being actively measured by new missions such as JWST and Gaia, and in the future HWO, ARIEL, and PLATO.

This material is based upon work supported by NASA'S Interdisciplinary Consortia for Astrobiology Research (NNH19ZDA001N-ICAR) under award number 19-ICAR19_2-0041.

References

Aguichine, A. 2024, Research Notes of the AAS, 8, 216

Aguichine, A. 2025, an0wen/MARDIGRAS: Upgrade to v2!

Aguichine, A., Batalha, N., Fortney, J. J., et al. 2025, ApJ, 988, 186

Aguichine, A., Fortney, J., Batalha, N., et al. 2025, Evolutionary tracks for Steam Worlds

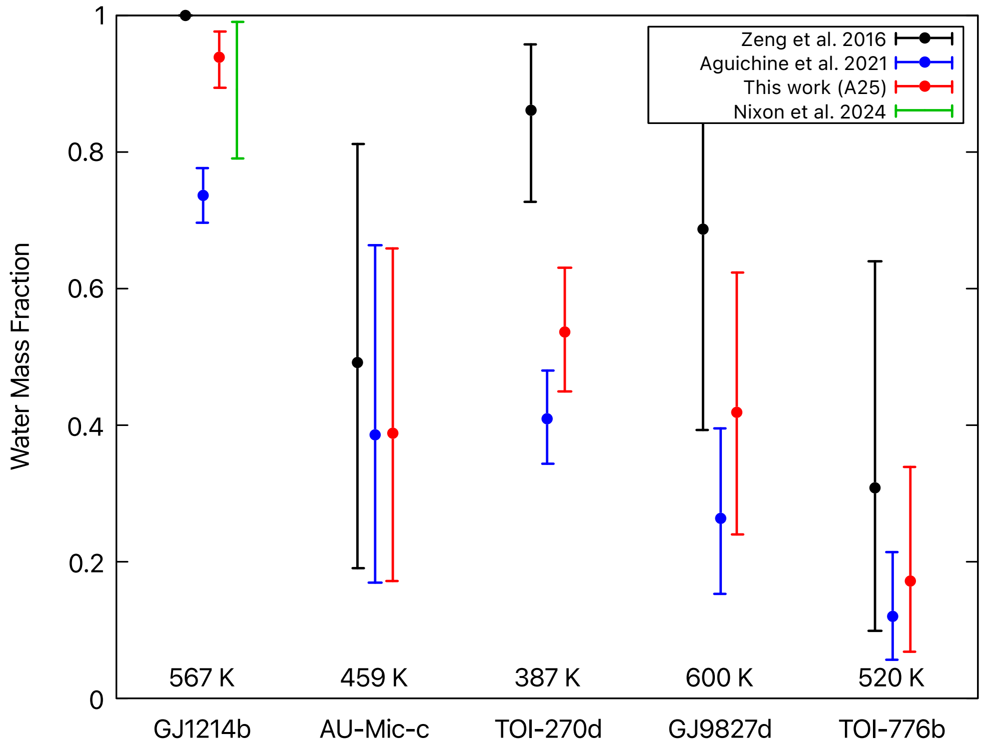

Fig. 2. Inferred water mass fraction of 5 exoplanets, 4 of which have been observed with JWST and found to have high mean molecular weight atmospheres. The WMF were inferred using the Z16 (Zeng et al. 2016), A21 (Aguichine et al. 2021) and A25 (this work) models. Green values correspond to the range of WMF inferred by the model of Nixon et al. (2024). Planets were ordered by decreasing central value of planetary radius.

Aguichine, A., Mousis, O., Deleuil, M., & Marcq, E. 2021, ApJ, 914, 84
Brugger, B., Mousis, O., Deleuil, M., & Deschamps, F. 2017, ApJ, 850, 93
Foreman-Mackey, D., Conley, A., Meierjurgen Farr, W., et al. 2013, emcee: The MCMC Hammer, Astrophysics Source Code Library, record ascl:1303.002
Fortney, J. J., Marley, M. S., & Barnes, J. W. 2007, ApJ, 659, 1661
Kempton, E. M. R., Lessard, M., Malik, M., et al. 2023, ApJ, 953, 57
Lopez, E. D. & Fortney, J. J. 2014, ApJ, 792, 1
Lopez, E. D., Fortney, J. J., & Miller, N. 2012, ApJ, 761, 59
Malik, M., Grosheintz, L., Mendonça, J. M., et al. 2017, AJ, 153, 56
Malik, M., Kempton, E. M. R., Koll, D. D. B., et al. 2019a, ApJ, 886, 142
Malik, M., Kitzmann, D., Mendonça, J. M., et al. 2019b, AJ, 157, 170
Mazevet, S., Licari, A., Chabrier, G., & Potekhin, A. Y. 2019, A&A, 621, A128
Mousis, O., Aguichine, A., Atkinson, D. H., et al. 2020a, Space Sci. Rev., 216, 77
Mousis, O., Deleuil, M., Aguichine, A., et al. 2020b, ApJ, 896, L22
Nakajima, S., Hayashi, Y.-Y., & Abe, Y. 1992, Journal of the Atmospheric Sciences, 49, 2256
Nettelmann, N., Fortney, J. J., Kramm, U., & Redmer, R. 2011, ApJ, 733, 2
Nixon, M. C., Piette, A. A. A., Kempton, E. M. R., et al. 2024, ApJ, 970, L28
Seager, S., Kuchner, M., Hier-Majumder, C. A., & Militzer, B. 2007, ApJ, 669, 1279
Tang, Y., Fortney, J. J., Nimmo, F., et al. 2024, arXiv e-prints, arXiv:2410.21584
Turbet, M., Bolmont, E., Ehrenreich, D., et al. 2020, A&A, 638, A41
Turbet, M., Ehrenreich, D., Lovis, C., Bolmont, E., & Fauchez, T. 2019, A&A, 628, A12
Valencia, D., Sasselov, D. D., & O'Connell, R. J. 2007, ApJ, 656, 545
Zeng, L., Jacobsen, S. B., Sasselov, D. D., et al. 2019, Proceedings of the National Academy of Science, 116, 9723
Zeng, L., Sasselov, D. D., & Jacobsen, S. B. 2016, ApJ, 819, 127